CFD INVESTIGATION AND EVALUATION OF EMISSION PRODUCTION OF A DIESEL POWER GENERATING PLANT

Ajoko Tolumoye John
Department of Mechanical Engineering
Faculty of Engineering, Niger Delta University, Wilberforce Island
Bayelsa State, **NIGERIA**
johntolumye@yahoo.co.uk, or
tjajoko@ndu.edu.ng

Otuami Obiga
Department of Mechanical Engineering, Faculty of Engineering
Niger Delta University, Wilberforce Island, Bayelsa State
NIGERIA
otubaba273@gmail.com

Umoren Goodnews Godwin
Department of Mechanical Engineering, Faculty of Engineering, Niger Delta University, Wilberforce Island
Bayelsa State, **NIGERIA**
goodnewsgodwin@gmail.com

ABSTRACT

Exhaust emissions from fossil fuel is a ticking time bomb to the environment. The continuous dependence on this black gold resources has generated serious catastrophe to the atmosphere. Thus, this concern is one motiving factor for the presentation of this paper. The study is enhanced by the application of computational fluid dynamics (CFD) in the investigation and evaluation of pollutants in the use of fossil fuel in power generating sets. Established results confirms high rate of NO_x production from diesel fuels. Deduced from the simulation are results from three different geometries analyzed are presented on residual and Contour plots. In all optimizing the combustion chamber (CC) by geometric modification of the combustion domain will reduce the production of NO_x.

Keywords: CFD, Combustion Chamber, Emission, Pollutant, Residuals.

INTRODUCTION

Human induced activities in the environment over the past decades has affected the climatic condition; thus given rise to depletion of the ozone layer, generation of greenhouse gas (GHG) and other toxic emissions. Hence, this paper presentation is to evaluation the level of emissions generation in diesel power plants. It is reported that NO_x production is mostly as a result of unburnt or incomplete combustion of diesel fuel used in diesel engines. Over 90% of the NO_x produced is by resource of the stationary combustion plants (Selvam et al., 2016). Likewise, the configuration of the combustion equipment significantly affects the rate of NO_x formation. Hence, NO_x emission factor for the normal combustion is about 46% higher than that for tangential combustion. Therefore, an internal combustion engine (ICE) with the use of diesel fuel emits a high factor of NO_x production up to 19-times as that in a tangentially fired boiler. Similarly, the NO_x emitted by turbines using diesel fuel is up to four times that of an external tangentially fired boilers (Samudra et al., 2014).

Conversely, another environmentally discharged pollutant causing serious concern is the carbon dioxide (CO_2). This makes up the vast majority of global GHGs (US EPA, 2019). Contributions from other researchers about the traces of CO_2 emissions present in the atmosphere as a result of the burning of fossil fuel is about 63% (Alhajeri et al., 2019; Heede, 2014). However, sulphur dioxide (SO_2) emissions are directly proportional to the sulfur content in the fuel, and the quantity of fuel consumed. Therefore, the accuracy of the SO_2 estimates depends on the degree of precision with which sulphur content in the fuel is reported (Samudra et al., 2014). Meanwhile, a scholarly report affirms that thermal power plants are responsible for 59% and 50% of the total atmospheric SO_2 emissions in the U.S. and India respectively (IIASA, 2012). Although, generation of electricity in the US accounts for closely 40% of CO_2

emissions from fossil fuelled power plants with a negative rise in the economic sector with the largest source (Pe´tron et al., 2008). Consequently, a reviewed literature attest that GHG effects are of 55% CO_2, 24% halocarbons refrigerants such as the chloro-fluoro-carbons (CFC), 15% methane (CH_4), and 6% and nitrous oxide (N_2O) (Demirbas, 2008, Moazzem et al., 2012). All of these impose a serious threat to health and have been linked with adverse health related illness.

However, the investigation and evaluation of these emissive pollutants to the environment is the cause of the study and various tools are used to achieve results. One of such over the years is the CFD. This, according to research determines the overall engine performance inlet and exhaust operational variables of a system (Ugur 2005). Similarly, the progressive modelling of a four stroke engine with the use of open **field operation and manipulation** (Open-FOAM) software has the capability of simulating ICEs and evaluating pressure distribution, turbulent kinetic energy as well as heat transfer in the CC (Stefan, 2009). The effectiveness of CFD cannot be over emphasized. It is reported that it was used for an optimization study for the combination of genetic algorithm (GA) and artificial neural network (ANN) to enhance the intake port design of a spark-ignited (SI) engine with four control parameters (Sun et al., 2015). Hence, the investigation and evaluation of the level of exhaust emissions from diesel engines can be achieved by the application of CFD simulation tool.

ENGINE MODEL AND SPECIFICATION

Perkins 403D-15G engine model is selected for the study. The model is a compact of 3 cylinders, 1.1 litres diesel motor that runs at1800 rpm**.** It works at full or part-time for days or weeks at a time which needs only a change of oil at every 500 hours of use. The diesel engine uses diesel as its fuel in general and it is more efficient than gasoline engines. The model and specification of the study engine is presented in table 1 and figure 1 respectively.

Table 1: Perkins 403D-15G Diesel Engine Specifications

Model	403D-15G
Parameters	Specifications
Mechanical Output	12-16 kWm
Electrical Output	13-17 kVA (10-14 kWe)
Rated Speed	1800 rpm
Bore	84.0 mm
Stroke	90.0mm
Displacement	1.5 Litres
Aspiration	Natural Aspiration
Coolant Capacity	6.0 litres
Oil Capacity	6.0 litres
Rotation from Flywheel End	Anti-clockwise
Number of Cylinders	3
Compression Ratio	22.5:1
Combustion System	Indirect injection
Cycle	4 stroke
Cooling System	Liquid (Water Cooled)
Width	497.0 mm
Length	820.0 mm
Height	791.0 mm
Dry Weight	197.0kg

Figure 1: Perkins 403D-15G Diesel Generator
Sources: (Perkins, 2019)

APPLICATION OF CFD SIMULATION TOOL

The CFD interface simulate experiments to determine approximate solutions. This is done in stages such as creation of geometry, mesh discretization, boundary specification selection, initialization of solution, computation of results and analysis. Following these steps, a cut out section of the CC of the study engine in figure 2 is analyzed. The combustion system of the diesel engine consists of a CC that is operated as a coaxial, a fuel inlet, air inlet and an exhaust outlet. The bore diameter and stroke length used in this analysis are specified by the manufacturer of engine as provided in the engine specification as 84 mm and 90 mm, respectively.

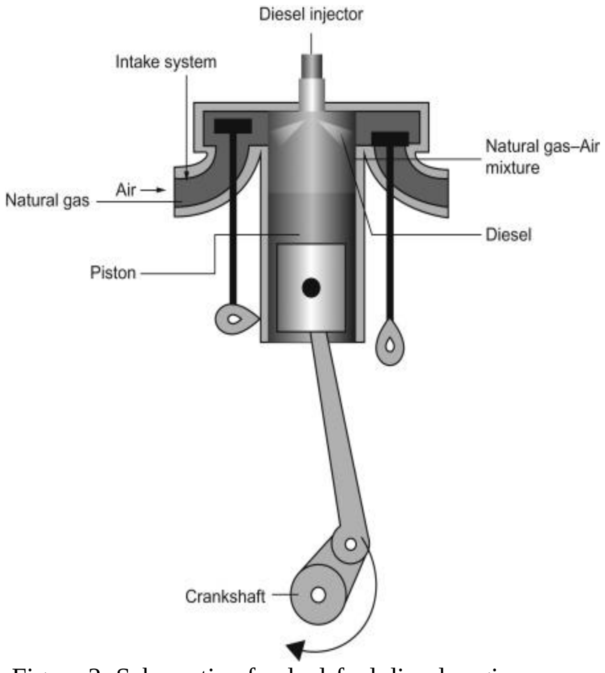

Figure 2: Schematic of a dual-fuel diesel engine

Meanwhile, the geometric configuration and dimensions of the CC used for the CFD simulation of the diesel engine combustion was carried out in Solidworks interface as shown in figure 3 and saved as IGES file format. This is to maintain CFD Ansys –Solidworks compatibility and easy import of files which is necessary for the operating system version used.

Conversely, tetrahedrons meshing with the Ansys Fluent solver is adopted for mesh discretization with an element size of 3.0e-002 m. After the process about 5332 number of elements with 14373 numbers of nodes was realized. The performance of discretization is necessary and important because at each point on the geometry there is a significant difference in parameter value during simulation**.** Thus, figure 4 presents the mesh information of the simulation.

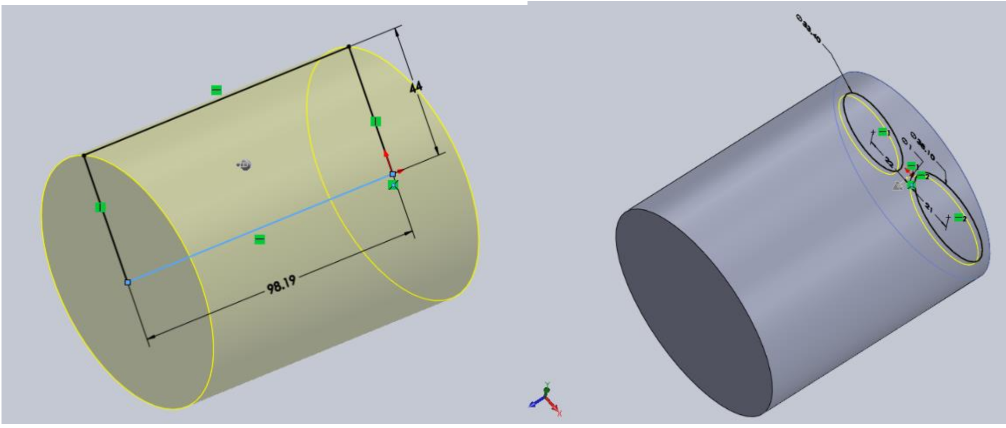

Figure 3: Geometry modelling using Solidworks 2013

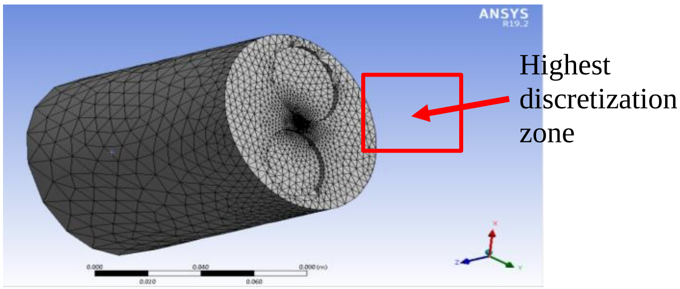

Figure 4: Discretized model of the combustion chamber

Consequently, upon the meshing process above, the following output was achieved; 76697 tetrahedral cells, zone 3, 5332 triangular wall faces, zone 1, 150478 triangular interior faces, zone 2, 324 triangular mass-flow-inlet faces, zone 6, 114 triangular mass-flow-inlet faces, zone 7, 62 triangular pressure-outlet faces, zone 8, 14373 nodes, and 14373 node flags. However, the simulation setup and boundary conditions were set at different inlets and outlet location and limit as well as the wall. Thus, the CFD Fluent simulation is governed by fluid flow equation – continuity, momentum, enthalpy, temperature, species mass fraction. Others are the k-epsilon model that estimates the turbulent-flow behaviour of the combustion, the turbulent dissipation rate, momentum balance, energy balance, partial mass balances, as well as the P-1 radiation model considering the expansion of the radiation intensity which are all presented in equations 1 – 9.

Continuity Equation:

$$\frac{\delta \rho U}{\delta t} + \nabla \cdot \rho U = 0 \quad \text{……………………………………..……………………………1}$$

Momentum Equation:

$$\frac{\delta \rho U}{\delta t} + \nabla \cdot \rho U U = -\nabla p + \nabla \tau + \rho g \quad \text{……………………………………………...……..2}$$

Enthalpy Equation:

$$\frac{\delta \rho h}{\delta t} + \nabla \cdot \rho U = \nabla \cdot \lambda_e \nabla T - \nabla q_r + \nabla \cdot \sum_l p h_l (T) D_e \nabla m_l \quad \text{……………………......3}$$

Temperature equation:

$$\rho C_p \frac{dT}{dt} = \nabla \cdot \lambda_e \nabla T - V \cdot \sum_l \rho h_l(T) D_e \nabla m_l - \rho \sum_l \frac{dm_l}{dt} h_l(T) \quad \ldots\ldots\ldots\ldots 4$$

Species Mass Fraction Equation:

$$\frac{\delta \rho m_l}{\delta t} + \nabla \cdot \rho U m_l = \nabla \cdot D_e \rho \nabla m_l - R_l \quad \ldots\ldots\ldots\ldots 5$$

Turbulent Kinetic Energy (*k*) Equation

$$\frac{\delta(\rho k)}{\delta t} + \frac{\delta(\rho k u_i)}{\delta x_i} = \frac{\delta}{\delta x_j}\left[\left(\mu + \frac{\mu_t}{\sigma_k}\right)\frac{\delta k}{\delta x_j}\right] + P_k + P_b + \rho \in - Y_M + S_k \quad \ldots\ldots\ldots\ldots 6$$

Turbulent Dissipation rate ($\in$) equation

$$\frac{\delta(\rho \in)}{\delta t} + \frac{\delta(\rho \in u_i)}{\delta x_i} = \frac{\delta}{\delta x_j}\left[\left(\mu + \frac{\mu_t}{\sigma_\in}\right)\frac{\delta \in}{\delta x_j}\right] + C_{1\in}\frac{\in}{k}(P_k + C_{3\in}P_b) - \rho C_{2\in}\frac{\in^2}{k} + S_\in \quad \ldots\ldots 7$$

P1 Radiation Model Theory:

$$-\nabla \cdot q_r = aG - 4an^2 \sigma T^4 \quad \ldots\ldots\ldots\ldots 8$$

Atomic mass fraction:

$$f = \frac{z_i - z_{i,OX}}{z_{i,fuel} - z_{i,OX}} \quad \ldots\ldots\ldots\ldots 9$$

RESULTS PRESENTATION AND DISCUSSION

The following set of results are obtained at the end of computational iteration of 1000. The study was conducted to determine the effect of change in the parametric analysis of the fuel as presented on table 2 which shows the stoichiometric flow rates. Likewise, presented on table 3 is a result summary of the CC of the ICE fuel characteristics. Other result presentations are shown graphically in figures 5 – 13.

Table 2: Stoichiometric Flow Rate

Fuel flow rate (kg/s)	Air flow rate (kg/s)	Excess Air (%)
3.38e – 04 Fuel Temperature (K) 353	7.93e – 03 Inlet Air Temp. (K) 298	0 Excess Air Temp (K) 298

Table 3: Results of Characteristics of Diesel Fuel of ICE

	NO ($x10^{-8}$)		N_2O ($x10^{-8}$)		N_2 ($x10^{-2}$)		CO_2 ($x10^{-2}$)		Static Temp. (k)		Radiation Temp. (k)	Turbulent Kinetic Energy (m^2/s^2)		Turbulent dissipation rate (Epsilon) (m^2/s^3)	
$G_{4.19}$	17	1.7	58.4	5.84	76.7	7.67	16.2	1.62	2200	296	1170	8570	4800	1.75E+10	1.05e–2
$G_{5.69}$	54.9	5.49	25.9	2.59	76.7	7.67	18.5	1.85	2150	297	1130	2320	3700	1.09E+09	5.96e–3
$G_{6.19}$	22.8	2.53	25.3	2.53	76.7	1.53	20.1	2.01	2330	296	9550	6350	1020	6.47E+09	1.48e–8

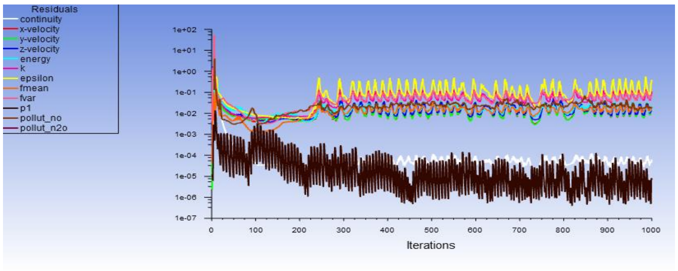

Figure 5: Residuals of $G_{4.19}$

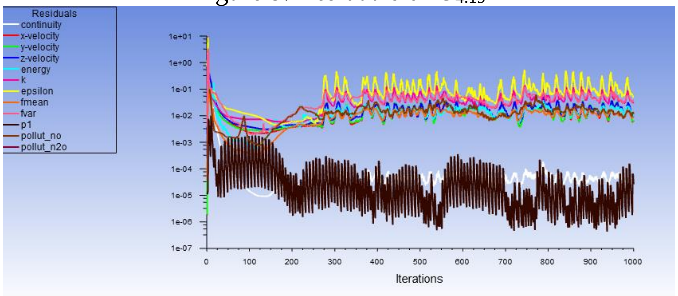

Figure 6: Residuals of $G_{5.69}$

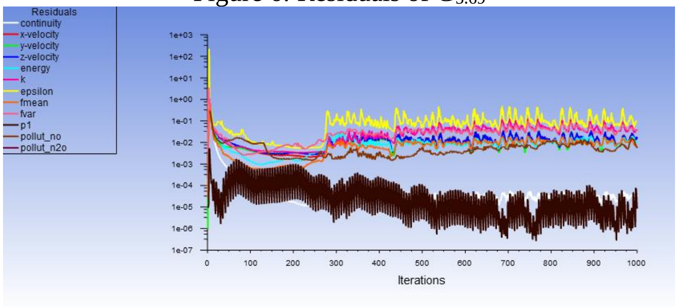

Figure 7: Residuals of $G_{6.19}$

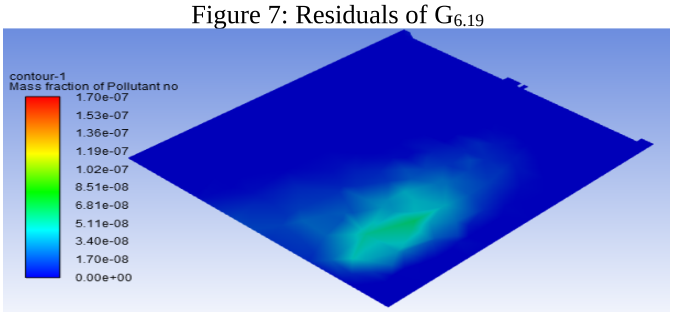

Figure 8: Contour plot of mass fraction of pollutant NO for $G_{4.19}$

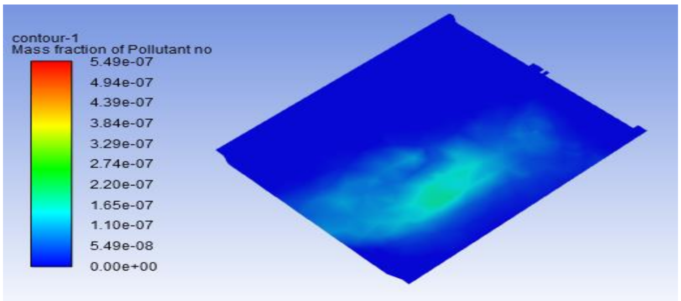

Figure 9: Contour plot of mass fraction of pollutant NO for $G_{5.69}$

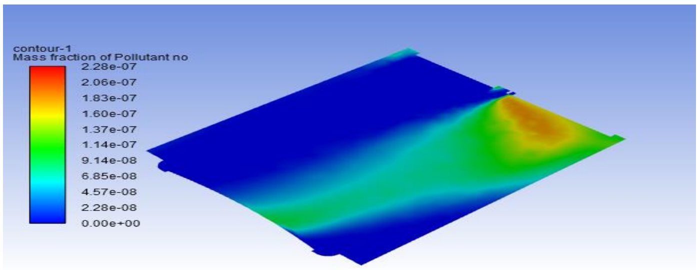

Figure 10: Contour plot of mass fraction of pollutant NO for $G_{6.19}$

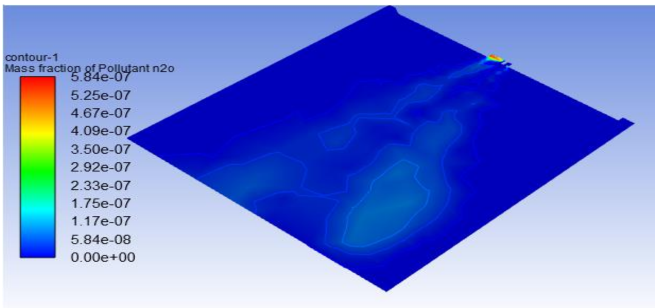

Figure 11: of mass fraction of pollutant N_2O for $G_{4.19}$

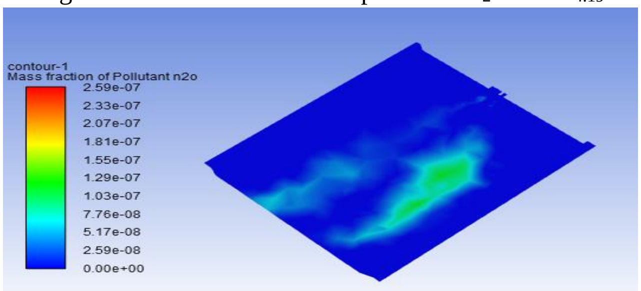

Figure 12: Contour plot of mass fraction of pollutant N_2O for $G_{5.69}$

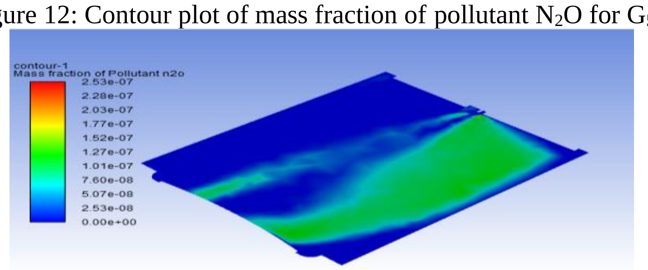

Figure 13: Contour plot of mass fraction of pollutant N_2O for $G_{6.19}$

Focusing in reducing the formation of NO_x and other pollutants leads to the optimization of the engine CC. Thus, this enables the determination and correlation between pollutant formation and CC geometry of the engine. Deduced from the simulation are three different geometries analyzed with the same input values of fuel, air properties and quantity. The results in table 3 shows the change in volume of the CC that it will inevitably result in the formation of more NO_x. The residual pollutants after the simulation are Nitric oxide (NO) and Nitrous oxide (N_2O). However, the temperature attained at combustion for $G_{4.19}$ and $G_{6.19}$, is 2200K and 2330K respectively which allows for thermal NO_x formation. Deducing from the formation of NO from the combustion of the three different piston crown geometry, $G_{5.69}$ produced the highest NO with 5.49e – 07 level, while $G_{4.19}$ produced the lowest emission value of 1.70e – 07. Relatively, the $G_{5.69}$ is 3.9% (9.00e - 07 m^3) more than $G_{4.19}$ by volume. The results display in figures 5 -7 shows residuals of the combustion process carried out on the piston crown geometry with clearance height of 4.19 mm, 5.69 mm and 6.19 mm respectively. The results attests that among the residuals, the NO and N_2O emissions has the highest level of pollutants production. However, the simulated maximum value of the contour plot for the mass fraction in figures 8 – 10 of NO pollutant for $G_{4.19}$, $G_{5.69}$ and $G_{6.19}$ are 1.7e-07, 5.49e-07 and 2.28e-07 respectively. It is observed that the formation of the NO pollutant is located at a tangible distance from the inlet, for both $G_{4.19}$ and $G_{5.69}$, whereas for $G_{6.19}$, the formation of NO is maximum at the inlet. This difference is due to the variance in the type of piston bowl geometry as confirmation of a reviewed literature.

Conversely, results in figure 11 shows the emission concentration of the pollutant N_2O for geometry $G_{4.19}$, with maximum mass fraction of 5.84e-07. Thus, the contour plot defines the location of the maximum mass fraction around the inlet, and a more concentration along the spray contour at distance from the inlet. Similarly, the N_2O formation for $G_{5.69}$ has a maximum mass fraction of 2.59e-07 located midpoint of the CC as shown in contour plot in Figure 12. Contrarily, the formation of N_2O for $G_{6.19}$ started from the inlet to the walls, and its maximum mass fraction is 2.53e-07. The variation value of the maximum mass fraction of N_2O is not as that for $G_{4.19}$ and $G_{5.69}$. However, it is being confirmed that amongst the exhaust pollutants from the combustion of diesel fuel, NO_x is the most occurring emission. This is in conformity with a scholarly research which justifies NOx prediction convergence to practical results depending on the physiochemical mechanism and the model sensitivity to input parameters.

CONCLUSION

The analysis of the combustion simulation performed on the study is for three different piston crown design with alteration on the CC geometry with the same cylinder design. A major consideration for optimization is the NOx formation in both direct and intermediate form, as well as other necessitating factors for the production of this pollutants. The Direct formation of NOx in the form of NO increases with increase in the size of the CC as well as increase in temperature, which is a function of the mixture fraction and mass flow rate. Therefore, in conclusion, the design of the piston crown should be based on its geometry and possibly modification of the combustion domain to reduce the production of NO_x.

REFERENCES

Alhajeri, N.S., Al-Fadhli, F.M. & Ahmed, Z. A. (2019). Unit-Based Emissions Inventory for Electric Power Systems in Kuwait: Current Status and Future Predictions. *Sustainability*, 11(5758), 1 – 19.

Demirbas, A. (2008). Carbon Dioxide Emissions and Carbonation Sensors Turkey, *Energy Sources*, Part A, 30, 70–78.

Heede, R. (2014). Tracing anthropogenic carbon dioxide and methane emissions to fossil fuel and cement producers, *Clim. Chang. 122*, 229–241.

International Institute for Applied Systems Analysis (IIASA) (2012). *GAINS Greenhouse Gas and Air Pollution Interactions and Synergies*. *Model Overview*. *IIASA South Asia Program 2012: Laxenburg, Austria*. [Accessed 15th November 2019]. Available from World Wide Web: https://gains.iiasa.ac.at/gains

Moazzem, S., Rasul, M.G. & Khan, M.M.K. (2012). *A Review on Technologies for Reducing CO2 Emission from Coal Fired Power Plants. Intechopen*, [Accessed 20th November 2019]. Available from World Wide Web: www.intechopen.com, 227 – 255.

Perkins (2019). *Perkins 403D-15G Diesel Engine [Online]*
[Accessed 27th December 2019]. Available from World Wide Web: *https://www.perkins.com › Perkins › Electric Power Generation › Diesel.*

Pe´tron, G., Tans, P., Frost, G., Chao, D. & Trainer, M. (2008). High-resolution emissions of CO2 from power generation in the USA. *Journal of Geophysical Research*, 113 G04008, doi:10.1029/2007JG000602

Samudra, V., Luisa, T.M. & Mario, J.M. (2014). *Estimating air Pollution Emissions from Fossil Fuel use in the Electricity sector in Mexico*. Unpublished Documentation for Integrated Program on Urban, Regional and Global air Pollution. *Massachusetts Institute of Technology, Mexico.*

Selvam, M., Selvam, R., Vigneshwaran, R., Irudhayaraj, R., Palani, S. & Parthasarathy, V. (2016). Emission Control Diesel Power Plant for Reducing Oxides of Nitrogen through Selective Catalytic Reduction Method using Ammonia. *Indian Journal of Science and Technology*. *9(1), 1-7.*

Stefan, G. (2009). CFD modeling of a four stroke S. I. engine for motorcycle application. Unpublished MSc. Thesis, KTH Industrial Engineering and Management, Stockholm, Sweden.

Sun, Y., Wang, T., Lu, Z. & Cui, L. (2015). The Optimization of Intake Port using Genetic Algorithm and Artificial Neural Network for Gasoline Engines. *SAE Technical Paper* 2015-01-1353

Ugur, K. (2005). Study on the design of inlet and exhaust system of a stationary internal combustion engine. *Elsevier-Energy Conversion and Management* 46(13-14), 2258–2287.

US EPA. (2019). *Global Greenhouse Gas Emissions Data.* US EPA:Washington, D.C. USA. Available online: https://www.epa.gov/ghgemissions/global-greenhouse-gas-emissions-data (accessed on 20th December, 2019).